A 70-kyr sea surface temperature record off southern Chile (Ocean Drilling Program Site 1233)

J. Kaiser
Deutsche Forschung Gemeinschaft Research Center Ocean Margins, University of Bremen, Bremen, Germany

F. Lamy
GeoForschungsZentrum-Potsdam, Potsdam, Germany

D. Hebbeln
Deutsche Forschung Gemeinschaft Research Center Ocean Margins, University of Bremen, Bremen, Germany

Received 15 February 2005; revised 27 May 2005; accepted 13 July 2005; published 29 October 2005.

[1] We present the first high-resolution alkenone-derived sea surface temperature (SST) reconstruction in the southeast Pacific (Ocean Drilling Program Site 1233) covering the major part of the last glacial period and the Holocene. The record shows a clear millennial-scale pattern that is very similar to climate fluctuations observed in Antarctic ice cores, suggesting that the Southern Hemisphere high-latitude climate changes extended into the midlatitudes, involving simultaneous changes in air temperatures over Antarctica, sea ice extent, extension of the Antarctic Circumpolar Current, and westerly atmospheric circulation. A comparison to other midlatitude surface ocean records suggests that this "Antarctic" millennial-scale pattern was probably a hemisphere-wide phenomenon. In addition, we performed SST gradient reconstructions over the complete latitudinal range of the Pacific Eastern Boundary Current System for different time intervals during the last 70 kyr. The main results suggest an equatorward displaced subtropical gyre circulation during marine isotope stages 2 and 4.

Citation: Kaiser, J., F. Lamy, and D. Hebbeln (2005), A 70-kyr sea surface temperature record off southern Chile (Ocean Drilling Program Site 1233), *Paleoceanography*, *20*, PA4009, doi:10.1029/2005PA001146.

1. Introduction

[2] While climate changes at millennial timescales during the last glacial period (marine isotope stages (MIS) 4 to 2) are relatively well known in the Northern Hemisphere (NH), there is a clear lack of records in the Southern Hemisphere (SH). Nevertheless, a number of new proxy records have been published over the last years and begin to provide a clearer picture of paleoceanographic pattern in the SH midlatitudes to high latitudes [e.g., *Charles et al.*, 1996; *Ninnemann et al.*, 1999; *Kanfoush et al.*, 2000; *Pahnke et al.*, 2003; *Lamy et al.*, 2004]. In the most widely accepted view, the primary trigger of millennial-scale changes on a global scale is located in the NH and involves abrupt changes in the global thermohaline circulation (THC), in particular in the formation of North Atlantic Deep Water (NADW) [e.g., *Rahmstorf*, 2002]. These changes result in large and abrupt climate shifts most clearly observed in the North Atlantic realm but also in other parts of the NH [e.g., *Voelker*, 2002]. The synchronization of ice cores from Antarctica and Greenland using methane concentrations provides strong evidence for a climatic seesaw pattern of the temperature changes in the NH and SH polar regions and the reconstruction suggests that the onset of seven major millennial-scale warmings in Antarctica preceded the onset of Greenland warmings [*Blunier and Brook*, 2001]. Many modeling studies provide evidence that this interhemispheric seesaw pattern could be largely induced by changes in NADW formation [e.g., *Rahmstorf*, 2002]. Other models suggest on the other hand that changes in temperature, sea ice extent and/or salinity around Antarctica could influence the strength of the North Atlantic THC [*Shin et al.*, 2003b] and possibly trigger abrupt events in the North Atlantic region as well [*Knorr and Lohmann*, 2003; *Weaver et al.*, 2003], which would support a more prominent role of the SH in abrupt climate changes. These different modeling results show that the ultimate mechanism behind short-term climate variability during the last glacial and the seesaw pattern still remains uncertain and high-resolution paleoceanographic records from the SH can greatly contribute to solving some of the open questions.

[3] Wherever the ultimate origin of millennial-scale climate and ocean variability is located, the surface eastern boundary currents along the western margins of the major continental landmasses act as conduits for the exchange of heat from the cold, high latitudes to the warm, low latitudes. The Peru-Chile Current (PCC), or Humboldt Current, is one of the largest and most productive Eastern Boundary Current systems in the world. Up to date, its spreading and functioning during the last glacial period is not well known because of the lack of records with sufficient resolution, especially in its southernmost part. Near the equator, recent studies suggest that during glacial maxima,

0883-8305/05/2005PA001146$12.00

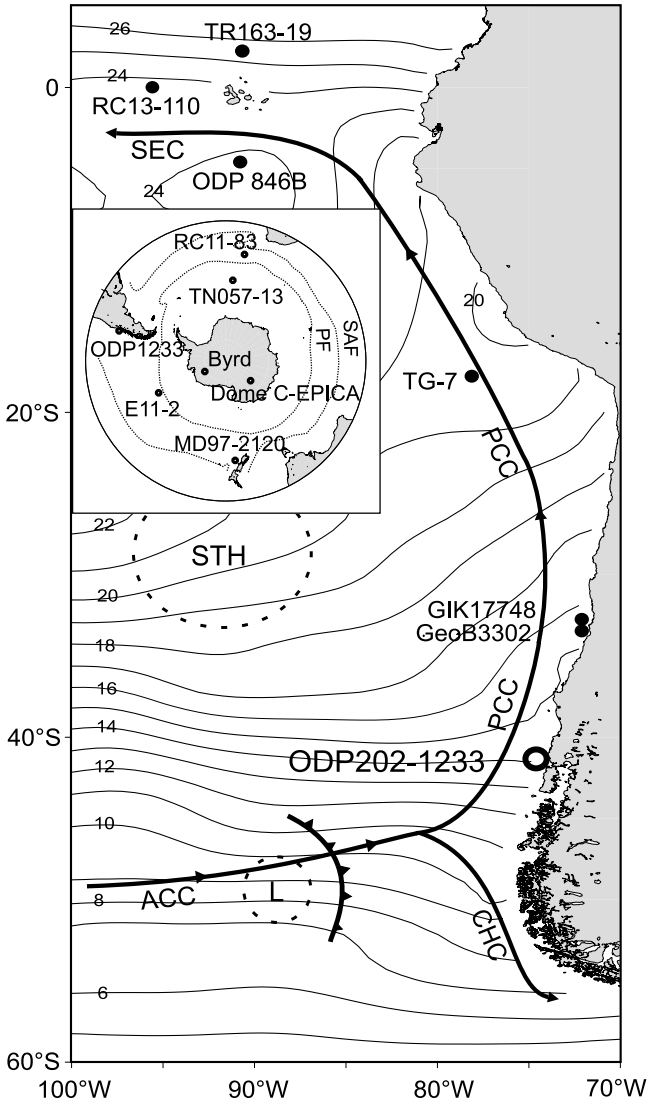

Figure 1. Modern annual mean sea surface temperature (SST) distribution (°C) [after *Levitus and Boyer*, 1994] in the southeast Pacific and the location of Ocean Drilling Program (ODP) Site 1233 (41°00′S, 74°27′W), as well as sediment cores discussed in the text: GeoB3302-1 (72°02′W, 33°13′S) [*Kim et al.*, 2002], GIK17748-2 (72°02′W, 32°45′S) [*Kim et al.*, 2002], TG-7 (78°60′W, 17°14′S) [*Calvo et al.*, 2001], ODP846B (90°49′W, 3°05′S) [*Martinez et al.*, 2003], RC13-110 (95°65′W, 0°09′N) [*Feldberg and Mix*, 2003], and TR163-19 (86°26′W, 2°12′N) [*Lea et al.*, 2000]. Abbreviations are ACC, Antarctic Circumpolar Current; CHC, Cape Horn Current; PCC, Peru-Chile Current; SEC, South Equatorial Current; STH, subtropical high pressure; and L, low-pressure belt associated with the westerlies. Inset shows location of the cores in the Southern Hemisphere midlatitudes to high latitudes used in the study (see Table 2). PF is Polar Front; SAF is Subantarctic Front.

the Pacific Eastern Boundary Current System (PEBCS) flow was stronger than today and thus substantially contributed to the cooling in the equatorial region [*Feldberg and Mix*, 2003; *Martinez et al.*, 2003].

[4] Southernmost South America is ideally located to reconstruct climate variability in the SH as it is situated under the influence of the dominant oceanographic (Antarctic Circumpolar Current, ACC) and atmospheric (westerly winds) circulation members. On land, extensive climate reconstructions mainly based on glaciological and palynological studies have shown the sensitivity of southernmost South America to climate changes since the Last Glacial Maximum (LGM) and during the Holocene [e.g., *Lowell et al.*, 1995; *Denton et al.*, 1999a, 1999b; *Moreno et al.*, 2001]. Some terrestrial records suggest a link to NH millennial-scale climate changes, such as a cooling during the NH Younger Dryas (YD) cold event [e.g., *Moreno et al.*, 2001], whereas others show no response to the YD [e.g., *Bennett et al.*, 2000]. Recently, *Lamy et al.* [2004] have presented high-resolution marine records in the southeast Pacific spanning the interval from 8 to 50 kyr. Contrary to reconstructions on the adjacent land, the record of past sea surface temperatures (SST) shows a clear millennial-scale "Antarctic timing" suggesting a close connection to SH high-latitude climate changes. On the basis of the record of iron concentrations of the same core, Lamy et al. proposed that the inertia of the Patagonian ice sheet to respond to rapid climate changes could partly explain the disagreements between land and ocean records.

[5] Here we present a high-resolution alkenone-based SST record from the SE Pacific midlatitudes off southern Chile (Ocean Drilling Project (ODP) Leg 202 Site 1233) covering the last ~70 kyr. SST and age model data are available at the World Data Center[1]. The study contains five main points: (1) the prolongation and improvement of the alkenone-based SST reconstruction published in the work of *Lamy et al.* [2004], which confirms our previous interpretations; (2) the improvement of the age model by tuning the SST to the oxygen isotope record of the Antarctic Byrd ice core between ~40 and 70 kyr; (3) the regional implications of the SST reconstruction for the southern PCC and adjacent southern South America; (4) a zonal comparison to other paleoceanographic records in the SH midlatitudes and a discussion of the possible forcing mechanisms at millennial to submillennial timescales during MIS 4 to 2; and (5) a latitudinal SST gradient reconstruction covering the complete PEBCS in order to better understand the different SST patterns and their implications for the atmospheric and oceanic circulations at different time intervals during the last glacial period and the Holocene.

2. Oceanographic and Atmospheric Settings

[6] The study area (Figure 1) is located at the northern margin of the ACC under the influence of cold, subantarctic surface waters and steep latitudinal SST gradients (~5°C between 43°S and 39°S) [from *Levitus and Boyer*, 1994].

[1] Auxiliary data are available electronically at the World Data Center for Marine and Environmental Sciences, Centre for Marine Environmental Sciences (MARUM), Klagenfurter Strasse, D-28359 Bremen, Germany (http://www.wdc-mare.org/PangaVista?query=@Ref26440).

Mean annual SSTs are around 14°C and the seasonal amplitude is ~5°C. The northern part of the ACC splits around ~43°S into the PCC flowing northward and the Cape Horn Current (CHC) turning toward the south [*Strub et al.*, 1998]. Subsurface currents at the core site include the southward flowing Gunther Undercurrent near the shelf edge, at depths of 100–300 m [*Fonseca*, 1989]. Between ~400 and ~1000 m, Antarctic Intermediate Water flows northward along the Chilean continental margin [*Strub et al.*, 1998].

[7] In the SE Pacific midlatitudes to high latitudes, the steepest SST gradient within the ACC is strongly related to the main atmospheric circulation member of the Southern Hemisphere, the westerly wind belt [*Streten and Zillman*, 1984]. This intense and powerful circulation, annually centered around 50°S, results from the strong thermal gradient and atmospheric pressure difference between cold air masses over Antarctica and the warmer air and water masses in the subtropical regions [*Cerveny*, 1998]. In southernmost South America, the westerlies and associated storm tracks bring heavy rainfalls, e.g., an annual mean greater than 2000 mm in Puerto Montt (41°S), and prevent upwelling south of 42°S [*Strub et al.*, 1998].

[8] *Trenberth* [1991] has described the modern seasonal fluctuation of the storm tracks associated to the westerlies in the Southern Hemisphere. In summer, the storm track activity can be as strong as in winter, but is located slightly equatorward of its winter position, and is concentrated in a tight band centered around 49°–50°S. In winter, storm track activity extends over a broader range of latitudes and is centered only 2° poleward from its summer position. The strong SST gradients associated with the ACC are marked by a northward latitudinal shift of ~5° in winter. The seasonal shifts of this coupled system are apparently controlled by seasonal changes in sea ice extent around Antarctica [*Markgraf et al.*, 1992], which has been estimated to range between 4 million km^2 in summer and 19 million km^2 in winter [*Comiso*, 2003].

[9] Site 1233 (41°S) is located at a key position to investigate the meridional oceanic heat exchanges in the southeast Pacific, i.e., at the origin of the PCC, the latitudinally most extensive Eastern Boundary Current system in the world, driven by south easterly winds along the Pacific coast of South America [*Strub et al.*, 1998]. The resulting offshore Ekman flow drives perennial upwelling of cool, nutrient-rich waters that produces one of the biologically most productive regions in the oceans [*Berger et al.*, 1987]. At about 5°S, the PCC is deflected offshore, feeds the South Equatorial Current (SEC) and flows westward as the equatorial cold tongue between 10°S and 4°N [*Wyrtki*, 1965]. North of the SEC, the Equatorial Front separates the cold, salty waters of the Peru-Chile Current from warmer and fresher tropical waters from the Northern Hemisphere. Thus the PCC acts as a conduit for exchange of heat and nutrients between high and low latitudes in the eastern Pacific.

3. Material and Methods

[10] Site 1233 was drilled during ODP Leg 202 off southern Chile (41°0.01′S, 74°26.99′W; 40 km offshore; 838 m water depth) in a small basin on the upper continental slope away from the pathway of major turbidity currents [*Mix et al.*, 2003]. Five Advanced Piston Corer holes were drilled at Site 1233 to ensure a complete stratigraphic overlap between cores from different holes. Detailed comparisons between high-resolution core-logging data performed shipboard demonstrated that the entire sedimentary sequence to 116.4 m below surface (mbsf) was recovered. On the basis of these data, a composite sequence (the so-called splice) was constructed representing 135.65 m composite depth (mcd).

[11] Sediments at Site 1233 are dominated by terrigenous components (clay and silty clay) with varying but generally small amounts of calcareous components (primarily nannofossils and foraminifera). Calcium carbonate concentrations and TOC contents range from 1 to 11 wt % (average = 5.4 wt %) and from 0.4 to 2.5 wt % (average = 0.9 wt %) [*Mix et al.*, 2003]. The TOC contents are substantially lower between 30 and 136 mcd (0.4 to 1 wt %) in comparison to the top of the core (up to 2.5 wt %). Samples for alkenone measurements were taken with intervals ranging from 12 to 149 cm (average = 61 cm) from the splice. Samples for ^{14}C accelerator mass spectrometry (AMS) dating were taken from outside the splice [*Lamy et al.*, 2004].

[12] To determine past SST variations off Chile, we have measured the alkenone unsaturation index UK'_{37} as defined by *Prahl and Wakeham* [1987] on 1–3 g freeze-dried and homogenized sediment samples. After the addition of internal standards [squalane ($C_{30}H_{62}$) and 2-nonadecanone ($C_{19}H_{38}O$)], alkenones were extracted using mixtures of methanol and methylene chloride with decreasing polarity (MeOH, MeOH/CH_2Cl_2 1:1, CH_2Cl_2) by ultrasonication (UP 200H sonic disruptor probe, Hielscher GmbH, 200W, 105μm amplitude, 0.5s pulse). After centrifuging, the extracts were combined, desalted with deionized water, dried with Na_2SO_4 and evaporated to dryness. The concentrated residue was dissolved in CH_2Cl_2. To avoid interferences with coeluting C_{36}-fatty acid methyl esters, saponification was performed using 0.1 N KOH in methanol (90/10 CH_3OH/H_2O) at 80°C for 2 hours followed by partitioning of the neutral fraction containing the alkenones into hexane. The extracts were finally concentrated under N_2 and taken up in 25 μL MeOH/CH_2Cl_2 (1:1).

[13] The extracts were analyzed by capillary gas chromatography using a HP 5890 series II Plus gas chromatograph equipped with a 60 m × 0.32 mm fused silica column (DB-5 MS, J&W) using split/splitless injection and a flame ionization detection. Helium was used as carrier gas with a constant pressure of 150 kPa. After injection at 50°C, the oven temperature was programmed to 250°C at a rate of 25°C/min, then to 290°C at a rate of 1°C/min, held for 26 min, and finally to 310 at a rate of 30°C/min, where the final temperature was maintained for 10 min.

[14] Quantification of the alkenones was achieved using HPGC ChemStation as analytical software. UK'_{37} was calculated from $UK'_{37} = (C_{37:2})/(C_{37:3} + C_{37:2})$, where $C_{37:2}$ and $C_{37:3}$ are the di- and tri-unsaturated C_{37} methyl alkenones. For conversion into temperature values, we used the culture calibration of *Prahl et al.* [1988] ($UK'_{37} = 0.034T + 0.039$), which has been validated by core top

compilations [*Müller et al.*, 1998]. The analytical precision was estimated to be around ±0.5°C. The SST estimate for the uppermost sample (14°C) matches the modern annual mean SST value for the core site [*Levitus and Boyer*, 1994]. This is in agreement with other alkenone temperature analyses of surface sediments recovered north of our study site [*Kim et al.*, 2002]. We thus consider that alkenone-derived SSTs correspond to the annual average of the ocean seawater surface. The alkenone content (defined as the sum of the $C_{37:3}$ and $C_{37:2}$ alkenones) ranges from ~2600 ng/g (between ~0 and 10 mcd) to ~700–1000 ng/g (for the rest of the core).

[15] It has been recently observed that alkenones may be substantially older than co-occurring planktic foraminifera [*Mollenhauer et al.*, 2005]. Holocene age differences measured on the Site 1233 survey core GeoB 3313-1 showed rather constant age offsets of ~1000 years. *Mollenhauer et al.* [2005] explained this offset as most likely resulting from continuous resuspension/redeposition cycles induced by internal tides and sediment focusing in morphologic depressions such as the small basin at Site 1233. By comparing the age offsets in different continental margin settings, they further noted that age offsets were largest where TOC contents and alkenone concentrations are highest. Therefore we expect that the age offsets if they are indeed induced by resuspension/redeposition cycles should be much smaller for the glacial section where both TOC and alkenone concentrations are significantly lower. We also note that grain-size data suggest constant and rather undisturbed fine-grained hemipelagic sedimentation (at least during the Holocene [see *Lamy et al.*, 2001]). Available oceanographic data show that bottom water circulation at the depth of Site 1233 (within the Antarctic Intermediate Water [e.g., *Shaffer et al.*, 2004]) is rather too sluggish for the resuspension of sediments and internal waves have not been described at the Chilean margin. Therefore it is likewise conceivable that a constant admixture of older material would affect the ^{14}C ages but not significantly the reconstructed alkenone temperatures, a possibility that *Mollenhauer et al.* [2005] did not exclude either.

[16] In some samples of the core (30 on a total of 223 samples), mainly located between ~30 and 80 mcd, the presence of coeluting organic compounds altered the peaks of the long-chain alkenones and thus the UK′37 values (Figure 2a top). To improve the measurements, liquid chromatography was applied to all the samples. The extracts were separated into three fractions by elution through a Bond silica column (Bond Elute column, Varian): (1) 4 mL of Hexane (apolar fraction), (2) 4 mL of a mixture of hexane and methylene chloride (3:1) (ketone fraction, including the alkenones) and (3) 2 mL of methylene chloride (alcohol fraction). Finally, all fractions were concentrated under N_2 and taken up in 25 μL $MeOH/CH_2Cl_2$ (1:1). The method was first tested on a reference sample and the UK′37 values obtained were within the estimated error bar (±0.056 UK′37, or 0.5°C). Figure 2a shows the gas chromatograms of the fractions containing the $C_{37:3}$ and $C_{37:2}$ alkenones and the organic compounds before (top plot) and after (bottom plot) liquid chromatography. A precise identification of the coeluting organic compounds using GC-MS is still unresolved (M. Elvert, personal communication, 2005) and is beyond the topic of the present study.

[17] The SSTs determined with this additional analytical step result in very similar UK37′ values as those obtained by *Lamy et al.* [2004] on the 10–90 mcd interval of the core. The correlation between both data sets is r = 0.98 (Figure 2b), and the highest SST differences occur at relatively low temperatures (8°–10°C). Only 13% of the data have significantly different SSTs (i.e., >0.5°C relative to the estimated methodological error; Figure 2 C), and mainly result in a shrinking of the extreme SST values. Therefore the interpretation of the previous published SST record is not significantly affected by our new data.

4. Stratigraphy

[18] The age model of the 135.7 mcd-long composite sequence at Site 1233 (Figure 3 and Table 1) has been constructed as follows. (1) The uppermost ~9 mcd have been correlated to the AMS ^{14}C dated gravity core GeoB 3313-1 from the same location [*Lamy et al.*, 2001] using magnetic susceptibility and Ca relative concentration records (Figure 3a). This correlation allowed us to transfer the age model of core GeoB 3313-1 (based on 7 AMS ^{14}C datings) to Site 1233. (2) Age control for the ~10 to ~70 mcd interval is provided by 17 AMS ^{14}C dates on mixed planktonic foraminifera samples [*Lamy et al.*, 2004] and the record of the Laschamp magnetic field excursion [*Lund et al.*, 2005]. All AMS ^{14}C dates were calibrated with the CALPAL software (available at www.calpal.de) using the CALPAL 2004 January calibration curve. We assume no regional deviation from the global reservoir effect of ~400 years because the core position lies significantly south of the Chilean upwelling zone and north of the southern polar front. Therefore the assumption of a 400 years reservoir age which is also the mean reservoir age for the Pacific Ocean at ~40°S appears to be the most reasonable assumption. For more details the reader can refer to the supporting online material of *Lamy et al.* [2004]. (3) As $\delta^{18}O$ data on planktic and benthic foraminifera are not yet available farther down hole, we propose here an updated and better constrained age model than that published by *Lamy et al.* [2004] for the older part of the record, i.e., below the Laschamp excursion, based on visual tuning. The millennial-scale SST variations in the AMS ^{14}C-dated part of the record closely follow Antarctic temperature fluctuations as recorded in the Byrd ice core [*Lamy et al.*, 2004] and the SST pattern farther down core shows a clear visible resemblance to the Antarctic record as well. Therefore we decided to tune our alkenone SST records to the Antarctic record using a minimum number of correlation points between our SST data set and the $\delta^{18}O$ record of the Byrd ice core (Figure 3b). For our purposes, the Byrd ice core has presently the most suitable age model for the last glaciation as it is linked to the Greenland GISP2 ice core record as well as our ^{14}C age calendar year conversion.

[19] The 135.7 mcd-long core covers the last ~70 kyr. The resulting mean sedimentation rates range between ~1.4 m/kyr in the Holocene to an average of ~2.2 m/kyr during MIS 4 to 2. These high sedimentation rates are

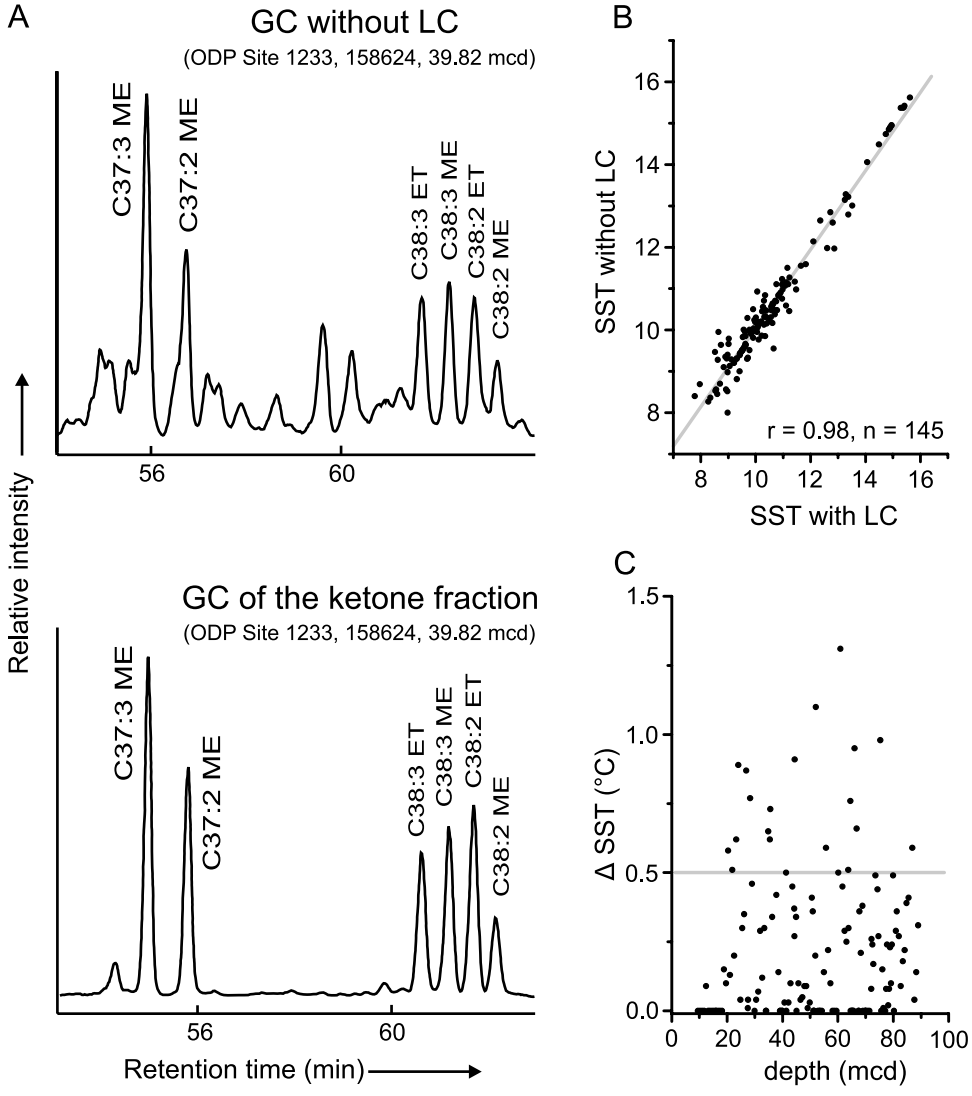

Figure 2. Effects of applying liquid chromatography (LC) to the extracts and comparison with previous published results. (a) Gas chromatogram (GC) of the GC window containing the C_{37} and C_{38} alkenones: whole fraction (top) without LC and (bottom) after LC (ketone fraction). (b) Correlation of SSTs based on measurements with (this study) and without LC (as published by *Lamy et al.* [2004]). (c) SST difference between the individual measurements. Only 13% of the data have significantly different SSTs (i.e., >0.5°C relative to the estimated methodological error).

consistent with strong fluvial discharge in response to heavy continental rainfall in southern Chile during the Holocene [*Lamy et al.*, 2001]. During the last glacial (MIS 2 to 4), the continental hinterland of Site 1233 was extensively glaciated as the Patagonian ice shield advanced toward the north [*Denton et al.*, 1999b] explaining even higher terrestrial input through glacial erosion processes [*Lamy et al.*, 2004].

5. Results and Discussion

5.1. SST Changes off Chile During the last 70 kyr: Results and Regional Aspects

[20] The alkenone-based sea surface temperature reconstruction at Site 1233 covers the last 70 kyr with a mean resolution of 320 years (Figure 3b) and thus provides the longest high-resolution SST record in the SE Pacific presently available. After a maximum of 14.7°C, probably corresponding to MIS 5.1, SSTs decrease to 8°C in MIS 4, the coldest temperatures of the record. Temperatures rise again up to ~12°C in early MIS 3 and display a general long-term cooling trend until ~45 kyr B.P. Superimposed on this trend, the major Antarctic warm events A2 to A4 [*Blunier and Brook*, 2001] are characterized by SST increases of up to 3°C. From 45 to 19 kyr B.P., the SSTs show millennial-scale variability of 2°–3°C around a mean temperature of 9.5°C. The LGM is not clearly defined in the record. *Denton et al.* [1999a] have reconstructed the summer mean air temperature in the adjacent Lake District region based on a combination of glacier fluctuations and pollen records spanning the last 60 kyr (not shown). Despite an apparent disagreement in the details of the timing of the terrestrial compared to the marine record in the SE Pacific

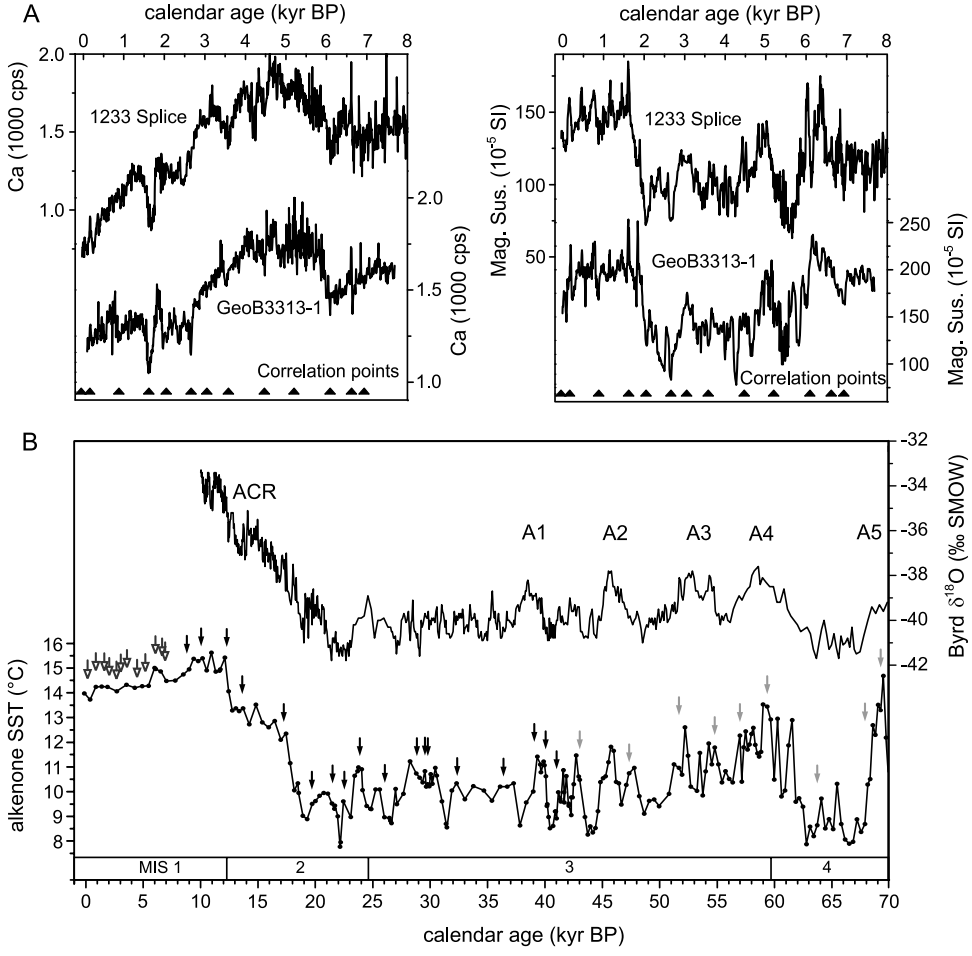

Figure 3. Age model of ODP Site 1233. (a) Correlation of Site 1233 to the ^{14}C-AMS dated core GeoB3313-3 [*Lamy et al.*, 2001] based on the magnetic susceptibility and Ca relative concentration records in the middle and late Holocene. (b) Alkenone-based SST reconstruction at Site 1233 compared to the Byrd δ^{18}O record over the last 70 kyr. The open arrows represent the correlation points to the core GeoB3313-1, the black arrows represent the ^{14}C-AMS datings and the Lashamp event at 41 kyr [*Lund et al.*, 2005], and the gray arrows show the tuning points to the oxygen isotope record of the Byrd ice core. A1 to A5 are Antarctic warm events after *Blunier and Brook* [2001]. ACR is Antarctic Cold Reversal; MIS is marine isotope stages 1 to 4.

[see *Lamy et al.*, 2004], their results are similar to our SST reconstruction in terms of main tendencies and amplitudes: ~8°C around 60 kyr B.P., an abrupt increase to 12°C at ~57 kyr B.P., decreasing values toward the LGM with temperatures around 8°C.

[21] A 6°C SST warming over Termination I is similar to results obtained from land, other marine records and modeling studies in the region. First, the previously cited summer air temperature reconstruction in the Lake District shows a 6°C warming over the last deglaciation. Second, two alkenone-based SST reconstruction farther to the north at 35°S and 33°S have a 6°C–7°C SST increase between 19 and 12.5 kyr B.P. [*Kim et al.*, 2002; O. Romero, preprint, 2005]. Third, in a recent modeling study of the changes in the Patagonian ice sheet extent during the LGM and the deglaciation, *Hulton et al.* [2002] have shown a good agreement between modeled ice extent and empirical evidence at the LGM by applying a temperature decrease of 6°C relative to present day. In our record termination I is interrupted by one major cooling event (~0.8°C) between 14.8 and 13.3 kyr B.P., followed by a plateau until 12.7 kyr B.P. (Figure 3b). This cooling matches the Antarctic Cold Reversal (ACR; 14 to 12.5 kyr B.P.) [e.g., *Jouzel et al.*, 1995] and clearly precedes the NH Younger Dryas (YD) (13–11.5 kyr B.P.) [e.g., *Rutter et al.*, 2000]. Instead, we observe a SST increase of 2.1°C during the early part of the YD (12.7 and 12.1 kyr B.P.) and early Holocene values thereafter. This pattern seems to be confirmed by two other alkenone-based SST records situated at 35°S and 30°S along the Chilean coast (O. Romero, preprint, 2005; J. Kaiser, unpublished data, 2005). On the basis of terrestrial records, the presence or absence of the NH YD in southern South America is discussed controversially. A cooling during the YD has been for example proposed from pollen records in NW Patagonia close to Site 1233 (Chilean Lake District region and Isla Grande de Chiloé) [e.g., *Denton et*

Table 1. Age-Depth Relation for ODP Site 1233[a]

Depth, mcd	^{14}C AMS Age, kyr	Plus/Minus Error, kyr	Calibrated Age, kyr cal. B.P.	Dating Method	Reference
0	-	-	−0.05	assumption 0 mcd = 2000 A.D.	this study
0.41	-	-	0.16	correlation to core GeoB 3313-1[b]	this study
1.45	-	-	0.88	correlation to core GeoB 3313-1[b]	this study
2.49	-	-	1.62	correlation to core GeoB 3313-1[b]	this study
3.19	-	-	2.05	correlation to core GeoB 3313-1[b]	this study
3.75	-	-	2.66	correlation to core GeoB 3313-1[b]	this study
3.99	-	-	3.05	correlation to core GeoB 3313-1[b]	this study
4.35	-	-	3.58	correlation to core GeoB 3313-1[b]	this study
5.28	-	-	4.47	correlation to core GeoB 3313-1[b]	this study
6.1	-	-	5.2	correlation to core GeoB 3313-1[b]	this study
7.7	-	-	6.09	correlation to core GeoB 3313-1[b]	this study
8.42	-	-	6.62	correlation to core GeoB 3313-1[b]	this study
8.86	-	-	6.93	correlation to core GeoB 3313-1[b]	this study
10.55	8.3	0.06	8.78	^{14}C AMS	*Lamy et al.* [2004]
12.94	9.34	0.08	10.04	^{14}C AMS	*Lamy et al.* [2004]
17.01	10.8	0.07	12.26	^{14}C AMS	*Lamy et al.* [2004]
20.22	12.28	0.07	13.62	^{14}C AMS	*Lamy et al.* [2004]
25.1	14.42	0.11	17.24	^{14}C AMS	*Lamy et al.* [2004]
29.81	17.07	0.11	19.68	^{14}C AMS	*Lamy et al.* [2004]
33.51	18.52	0.13	21.48	^{14}C AMS	*Lamy et al.* [2004]
36.56	19.74	0.14	22.51	^{14}C AMS	*Lamy et al.* [2004]
39.5	21.08	0.15	23.86	^{14}C AMS	*Lamy et al.* [2004]
43.72	22.93	0.23	26.05	^{14}C AMS	*Lamy et al.* [2004]
47.25	25.28	0.24	28.83	^{14}C AMS	*Lamy et al.* [2004]
49.11	26.1	0.29	29.51	^{14}C AMS	*Lamy et al.* [2004]
50.72	26.52	0.3	29.78	^{14}C AMS	*Lamy et al.* [2004]
55.02	29.03	0.39	32.34	^{14}C AMS	*Lamy et al.* [2004]
59.03	32.19	0.58	36.36	^{14}C AMS	*Lamy et al.* [2004]
62.5	34.48	0.75	39.05	^{14}C AMS	*Lamy et al.* [2004]
64.81	35.77	0.79	40.02	^{14}C AMS	*Lamy et al.* [2004]
67.8	-	-	41	paleomagnetic age (Laschamp event)	*Lund et al.* [2005]
74.62	-	-	43.01	SST tuned on Byrd δ^{18}O	this study
81.25	-	-	47.31	SST tuned on Byrd δ^{18}O	this study
88.26	-	-	51.65	SST tuned on Byrd δ^{18}O	this study
96.66	-	-	54.76	SST tuned on Byrd δ^{18}O	this study
101.55	-	-	56.95	SST tuned on Byrd δ^{18}O	this study
111.36	-	-	59.31	SST tuned on Byrd δ^{18}O	this study
121.17	-	-	63.7	SST tuned on Byrd δ^{18}O	this study
129.56	-	-	67.84	SST tuned on Byrd δ^{18}O	this study
133.75	-	-	69.21	SST tuned on Byrd δ^{18}O	this study

[a]All radiocarbon ages are calibrated using the CALPAL 2004 January calibration curve (available at www.calpal.de) and a constant reservoir age correction of 400 years (see section 4 for details); mcd is meters composite depth.

[b]Correlation to the ^{14}C AMS-dated core GeoB 3313-1 from the same location [*Lamy et al.*, 2001] using the magnetic susceptibility and Ca relative concentration records.

al., 1999a; *Moreno et al.*, 2001] and seems to be present in subantarctic Patagonia as well [*Heusser et al.*, 2000; *Massaferro and Brooks*, 2002]. However, it has been recently suggested that the deglacial cold reversal in NW Patagonia started earlier (at ∼14.7 to 13.4 kyr B.P.), and that the YD interval is rather characterized by fire disturbances [*Hajdas et al.*, 2003; *Moreno*, 2004] that may not necessarily imply cooling. In addition, other paleoenvironmental reconstructions in southern Chile (∼40°S to 48°S) based on pollen, glacial morphology, and beetle assemblages did not find evidence of a cooling during the YD epoch either [e.g., *Ashworth and Hoganson*, 1993; *Bennett et al.*, 2000; *Glasser et al.*, 2004].

[22] The SSTs reach a maximum of 15.6°C in the early Holocene (∼11 to 9 kyr B.P.) and generally decrease thereafter, reaching the modern SST (∼14°C) in the late Holocene (Figure 3b). A warmer and drier-than-today climate over southwestern South America in the early Holocene was also recorded on the adjacent land [e.g., *Massaferro and Brooks*, 2002; *Moreno and León*, 2003; *Abarzúa et al.*, 2004], and even in the low latitudes, e.g., in the Huascaràn ice core [*Thompson et al.*, 1995]. Furthermore, most Antarctic ice core records show a widespread early Holocene optimum between 11.5 and 9 kyr B.P. [*Masson et al.*, 2000]. This early Holocene optimum was not documented in the earlier SST record based on the short core (GeoB 3313-1 [*Lamy et al.*, 2001]) drilled at the same location as Site 1233 that only covers the last ∼8 kyr. Details on millennial to multicentennial-scale variations during the middle and late Holocene can be found in the work of *Lamy et al.* [2002].

[23] Holocene and glacial climate fluctuations in the SE Pacific region and adjacent South America have often been related to changes in the latitudinal position of the SH westerlies and a northward shift of this wind belt has been proposed for this region based on a number of terrestrial and marine archives [e.g., *Heusser*, 1989; *Lamy et al.*, 1998; *Benn and Clapperton*, 2000; *Moreno and León*, 2003].

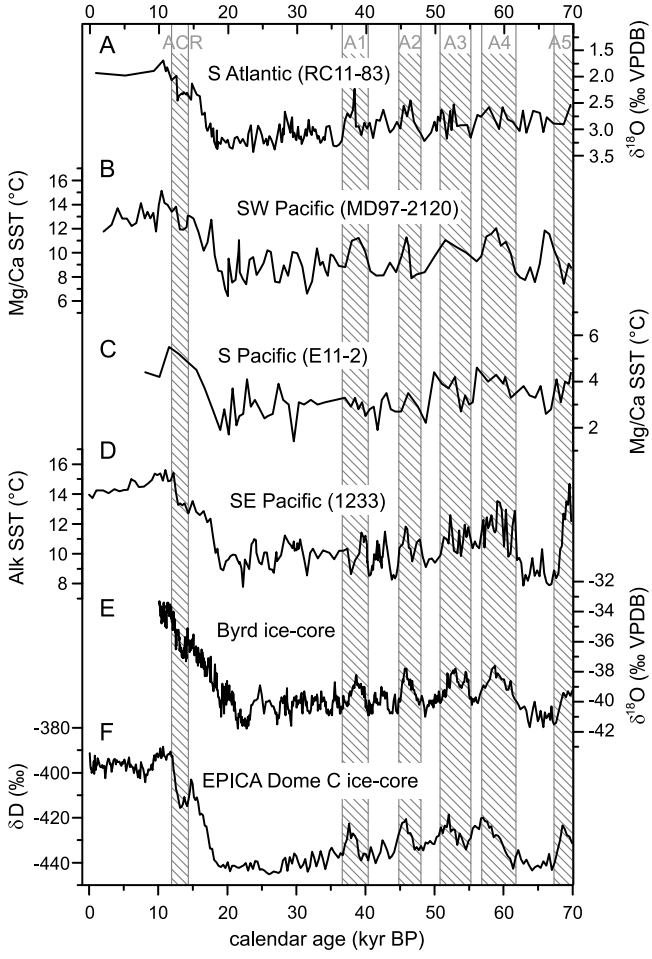

Figure 4. Comparison of the Site 1233 SST record in the SE Pacific with other SST proxy records from the Southern Hemisphere, and the Antarctic air temperature records of Byrd and European Programme for Ice Coring in Antarctica (EPICA) Dome C ice cores, during the past 70 kyr. (a) Oxygen isotope record on planktic foraminifera in the South Atlantic [*Ninnemann et al.*, 1999]. (b) Mg/Ca SST reconstruction in the southwest Pacific [*Pahnke et al.*, 2003]. (c) Mg/Ca SST reconstruction in the South Pacific [*Mashiotta et al.*, 1999]. (d) Alkenone SST reconstruction at ODP Site 1233 (this study). (e) Oxygen isotope record of the Byrd ice core [*Blunier and Brook*, 2001]. (f) Deuterium profile from the EPICA Dome C ice core [*EPICA Community Members*, 2004]. ACR is Antarctic cold reversal; A1 to A5 indicate Antarctic warm events after *Blunier and Brook* [2001]. See Figure 1 for the location of the cores.

Together with the westerlies, the ACC was apparently displaced northward at the LGM as well. High paleoproductivity at ~33°S off Chile during the LGM suggests that an equatorward shift of the ACC would have brought the main nutrient source closer to the core sites resulting in increased productivity [*Hebbeln et al.*, 2002; *Mohtadi and Hebbeln*, 2004]. We note that a northward displacement of the westerlies during the LGM is in disagreement with some other paleoenvironmental records [e.g., *Markgraf et al.*, 1992] as well as with modeling results [*Wyrwoll et al.*, 2000; *Wardle*, 2003] that suggest little latitudinal change or even a slight poleward shift. Nevertheless, *Wyrwoll et al.* [2000] point out that associated with the southward shift and increase westerly flow around 60°S, there was a distinct widening of the zone of strong westerlies, similar to the modern winter conditions (see section 2). Taken together, the overall regional proxy evidences strongly suggest that the SST variability at Site 1233 was predominantly caused by latitudinal shifts of the ACC and the southern westerlies (or their northern boundary), i.e., cold temperatures associated with a northward shift of the coupled system and vice versa.

5.2. Surface Water Changes in the SH Midlatitudes: Toward a Common Millennial-Scale Pattern and Associated Forcing Mechanisms

[24] The close resemblance of SST changes at Site 1233 to Antarctic temperature changes within the ^{14}C-AMS dated section and the very similar temperature pattern in the earlier part of the records, allowed us to transfer the Byrd age model to Site 1233 for the older interval (see section 3). Our new results are thus prolonging the previously discussed pattern of close climate linkages between the SH midlatitudes and high latitudes [*Lamy et al.*, 2004] into late MIS 5. In Figure 4, our 70 kyr SST record off southern Chile is compared with other records of changes in surface water properties in the SH midlatitudes (see Figure 1 for site locations): an oxygen isotope record of *Globigerina bulloides* in the South Atlantic [*Ninnemann et al.*, 1999] and two Mg/Ca SST records, one from the southwest Pacific [*Pahnke et al.*, 2003] and a second from the central south Pacific [*Mashiotta et al.*, 1999]. The ^{14}C-based parts of the age models were recalculated with the CALPAL January 2004 calibration curve. A recalibration was not possible for the record in the central South Pacific [*Mashiotta et al.*, 1999], that is based on tuning (see Table 2). Considering the errors of dating and the differences in the mean resolutions (between 350 and 920 years), the records present a common pattern which is very similar to the Antarctic Byrd δ^{18}O and the recent EPICA δ deuterium records (Figures 4e–4f): warmer SSTs during the Antarctic warm events A1 to A4 (as defined by *Blunier and Brook*, [2001]), a 4°C to 6°C warming over termination I, beginning simultaneously around 19 kyr B.P., the record of the Antarctic Cold Reversal (except in the south Pacific, most likely because of the low resolution of the record), and finally a Holocene climatic optimum between ~9 and ~11 kyr B.P. This common pattern suggests that Antarctic climate changes extended into the SH midlatitudes involving changes in the ACC and the westerlies. The most likely mechanism is a common latitudinal shift of the coupled system, i.e., equatorward during cold phases and poleward during warm intervals. Assuming a global mean LGM cooling of ~2°C as predicted by a coupled ocean-atmosphere GCM model for the intertropical oceans [*Ganopolski et al.*, 1998] and that the remaining SST changes in the SE Pacific were mainly driven by coeval shifts of the westerlies (or their northern boundary) and the ACC during the last 70 kyr, it is possible to give a rough estimation of the latitudinal shifts when extrapolating from the modern SST pattern [after

Table 2. Modifications Made to the Published Age Models From Some Records Used in Figures 4 and 5[a]

Reference	Core	Location	Original Age Model	Modification for This Study
Ninnemann et al. [1999]	RC11-83	41°36′S, 9°48′E	^{14}C AMS dates (40 kyr to present)	new calibration with CALPAL 2004 January
			MIS 5/4 boundary based on SPECMAP chronology	no modification
Pahnke et al. [2003]	MD97-2120	45°32′S, 174°55′E	^{14}C AMS dates (35 kyr to present)	new calibration with CALPAL 2004 January
			benthic δ^{18}O tuned to benthic δ^{18}O of core MD95-2042 (72–35 kyr)	no modification
Mashiotta et al. [1999]	E11-2	56°04′S, 115°05′E	planktonic δ^{18}O correlated to planktonic δ^{18}O of core RC11-83 (40 kyr to present) and core RC11-120 (110–40 kyr) [after *Ninnemann and Charles*, 1997]	no modification
Shemesh et al. [2002]	TN057-13	53°20′S, 5°10′E	^{14}C AMS dates	new calibration with CALPAL 2004 January

[a]All other records coming from the literature presented in this study are plotted on their original age models.

Levitus and Boyer, 1994]. Our results suggest that the whole coupled system might have shifted northward by 4°–5° of latitude during the LGM. Applying the same assumptions to MIS 4 would result in a 5°–6° northward shift of the system. The estimated displacement for the LGM is consistent with the 5°–10° northward latitudinal expansion of Antarctic cold waters as recently suggested by *Gersonde et al.* [2005] and the 5° latitudinal shift of the westerlies as proposed by works in South America [*Heusser*, 1989; *Lamy et al.*, 1998; *Mohtadi and Hebbeln*, 2004]. On the other hand, a warmer-than-today climate during the early Holocene as suggested by the records of surface water changes would imply a southward shift of the coupled system. This is in agreement with most of the climate reconstructions on terrestrial and marine archives of the SH midlatitudes [e.g., *Brathauer and Abelmann*, 1999; *Moreno and León*, 2003; *Haberle and Bennett*, 2004; *Shulmeister et al.*, 2004].

[25] A dust content record from Antarctica provides additional evidence for a close coupling of atmospheric circulation around Antarctica and temperature changes in the SH midlatitudes at millennial timescales. In Figures 5c and 5d the SST record at Site 1233 is plotted against the dust content as measured on EPICA Dome C ice core [*Delmonte et al.*, 2002; *EPICA Community Members*, 2004]. The main origin of Antarctic dust is the Patagonian region in southernmost South America [*Grousset et al.*, 1992; *Basile et al.*, 1997]. The general increase in the dust contents during the coldest periods, i.e., MIS 4 and 2 in our case, has been explained by expanded source regions linked to the global sea level drop, a decrease of the vegetation and a general dryer climate in Patagonia [*Petit et al.*, 1981; *Delmonte et al.*, 2002]. Despite these pronounced long-term signal in the dust record, short-term variations on millennial and submillennial timescales appear to parallel the short-term variations in our SST record. Considering the offsets between 70 and 41 kyr B.P. induced by age model discrepancies between the EPICA Dome C and Byrd ice cores (Figures 5a and 5b) and the limitations in dating accuracy of our record (Figure 5d) as well as in the age models of the ice cores, we observe a reasonable correlation of high dust contents to millennial-scale SST cold peaks and conversely. Environmental changes in the source areas of the dust might have played a role in dust variability on millennial timescales [*Rothlisberger et al.*, 2002]. High-resolution palynological studies from Patagonia are unfortunately not yet available in order to proof this hypothesis. On the other hand, dust input maxima on millennial timescales could have been induced by intensified circumpolar winds probably linked to a strengthening of the polar vortex by a steeper latitudinal thermal gradient, generated by the northward extension of sea ice [*COHMAP*, 1988; *Delmonte et al.*, 2002]. A faster dust transport from Patagonia to Dome C during the LGM has also been proposed based on GCM simulations [*Krinner and Genthon*, 2003]. In addition, intensified SH westerlies during the LGM are suspected (but not proofed) in records of dust/loess and glacier advances in New Zealand (for a review see *Shulmeister et al.* [2004]) and are often proposed in simulations of a global LGM climate [e.g., *Wyrwoll et al.*, 2000; *Shin et al.*, 2003a]. It is thus conceivable that the millennial-scale SST variability in the SE Pacific was likewise linked to changes in the intensity of the westerlies in addition to the latitudinal shifts as discussed above.

[26] Recent modeling studies on the last deglaciation suggest that changes in sea ice extent and/or salinity in the Southern Ocean may have had large consequences for millennial-scale changes on a global scale [*Knorr and Lohmann*, 2003; *Weaver et al.*, 2003]. The involvement of sea ice extent changes in SH millennial-scale climate variability is consistent with the comparison of our SST record to an index of the sea ice presence during the last ~45 kyr in the South Atlantic [*Shemesh et al.*, 2002] (core TN057-13, location in Figure 1). The sea ice record suggests millennial-scale variations that imply, within the errors of dating, extended sea ice duration during the cold intervals in the southeast Pacific as shown by our data (Figures 5d and 5e). Therefore we suggest that the extended sea ice in the Southern Ocean displaced the ACC equatorward and triggered enhanced advection of cold, subantarctic surface waters into our study area. Furthermore, *Kanfoush et al.* [2003] improved the chronology of the ice-rafted detritus (IRD) record in the SE Atlantic [*Kanfoush et al.*, 2000] and concluded that major IRD events occurred during the cooling phases following the A1 to A4 warm events (not shown). It has been argued that the IRD events were associated with increased NADW production during major NH interstadials [*Kanfoush et al.*, 2000] what would be consistent with the bipolar seesaw mechanism [*Broecker*,

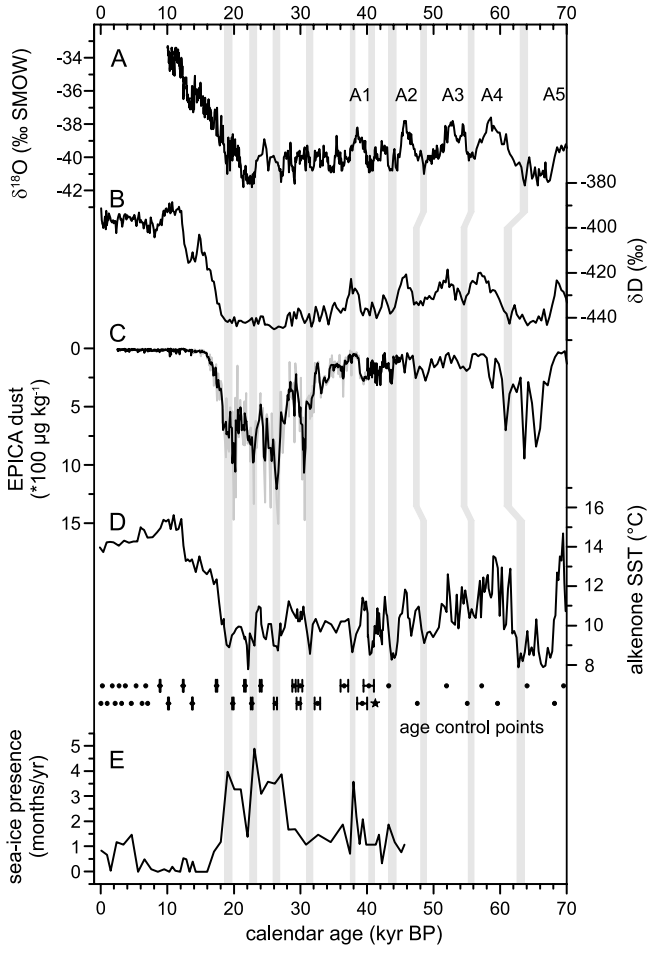

Figure 5. Relationship of the SE Pacific SST reconstruction and Southern Hemisphere high latitudes. (a) Oxygen isotope record of the Byrd ice core [*Blunier and Brook*, 2001]. (b) Deuterium record from the EPICA Dome C ice core [*EPICA Community Members*, 2004]. (c) EPICA Dome C dust content (plotted inverse) [*EPICA Community Members*, 2004; *Delmonte et al.*, 2002]. Original data (gray line) and 3-point moving average data between 15 and 35 kyr (black line). (d) Alkenone SST at Site 1233 (this study), plotted with the age control points of the core (see Table 1). (e) Sea ice presence reconstruction based on diatoms in the South Atlantic [*Shemesh et al.*, 2002] (core TN057-13, see Figure 1 for location). A1 to A5 are Antarctic warm events after *Blunier and Brook* [2001]. Note that the offsets between SST and EPICA Dome C dust records from 70 to 41 kyr are primarily due to the offset between Byrd $\delta^{18}O$ and EPICA δD records.

1998; *Stocker*, 1998; *Blunier and Brook*, 2001]. On the other hand, the middle to high southern latitude–wide millennial-scale pattern of surface ocean changes with Antarctic timing during the last ~70 kyr in all ocean basins (see Figure 4) is inconsistent with most modeling studies on the SH response to THC throttling or shutdown [*Ganopolski and Rahmstorf*, 2001; *Schmittner et al.*, 2003]. Therefore, as already discussed in relation to the ^{14}C-dated part of our record [*Lamy et al.*, 2004], it is equally conceivable that the millennial-scale changes are of SH origin.

[27] The emerging pattern of common millennial-scale climate and ocean changes in the SH midlatitudes and high latitudes suggests similar SST changes in the midlatitudes, most likely controlled by changes in the strength and latitudinal position (or extension) of the westerlies and the ACC. These variations appear to be closely linked to changes in Antarctic temperatures and the extent of sea ice as well. The paleorecords suggest a scenario that largely resembles the coupled atmosphere-ocean mechanisms linked to the Southern Annular Mode (SAM), an important modern mode of interannual to decadal-scale climate variability in the SH [*Thompson and Wallace*, 2000; *Thompson et al.*, 2000]. During a positive SAM, the surface temperature over Antarctica cools and the strength of the westerlies over the subpolar Southern Ocean increases [*Thompson and Wallace*, 2000]. Enhanced westerly winds could generate a northward Ekman flow advecting sea ice farther north, as proposed by a coarse resolution model [*Hall and Visbeck*, 2002], that would act as a positive feedback mechanism. Therefore we speculate that long-term changes in the interannual SH climate modes, such as the SAM, may ultimately be involved in millennial-scale ocean and atmosphere changes in the SH midlatitudes and high latitudes during the last glaciation.

5.3. SST Gradient Changes Along the Pacific Eastern Boundary Current System During the Last Glacial Period (MIS 4 to 2) and the Early Holocene

[28] On the basis of coupled ocean-atmosphere models, *Liu et al.* [2002] and *Shin et al.* [2003a] have proposed that the upper ocean circulation in the southern midlatitudes and high latitudes plays a key role in explaining tropical cooling at the LGM. A similar line of evidence comes from a number of paleoenvironmental reconstructions in the tropical eastern Pacific low latitudes. On the basis of a Mg/Ca SST reconstruction near the equator, *Lea et al.* [2000] have hypothesized a link between polar and tropical temperature changes because of some similarities with isotopic changes in Antarctic ice cores. High southern latitude foraminifera species were present even north of the equator suggesting an intensification of the Peru-Chile Current during the LGM [e.g., *Feldberg and Mix*, 2003; *Martinez et al.*, 2003]. Sea surface temperature reconstructions based on foraminiferal faunal assemblages have shown that the meridional SST gradient in the Eastern Equatorial Pacific (EEP) was stronger during the LGM, suggesting "La Niña-like" conditions [*Martinez et al.*, 2003]. Likewise, a reconstruction of zonal gradients in the tropical Pacific Ocean suggests a shallower thermocline with a steeper east-west slope resulting in an intensified Walker circulation during the LGM [*Andreasen and Ravelo*, 1997], as presently occurring during La Niña events. However, a reversed pattern for the LGM, i.e., "El Niño-like" conditions, has been proposed by other authors [*Koutavas et al.*, 2002].

[29] Our new SST record off southern Chile provides the opportunity to reconstruct paleoceanographic changes in the PEBCS in its middle- to low-latitude section during the last 70 kyr, based on a SST gradient reconstruction.

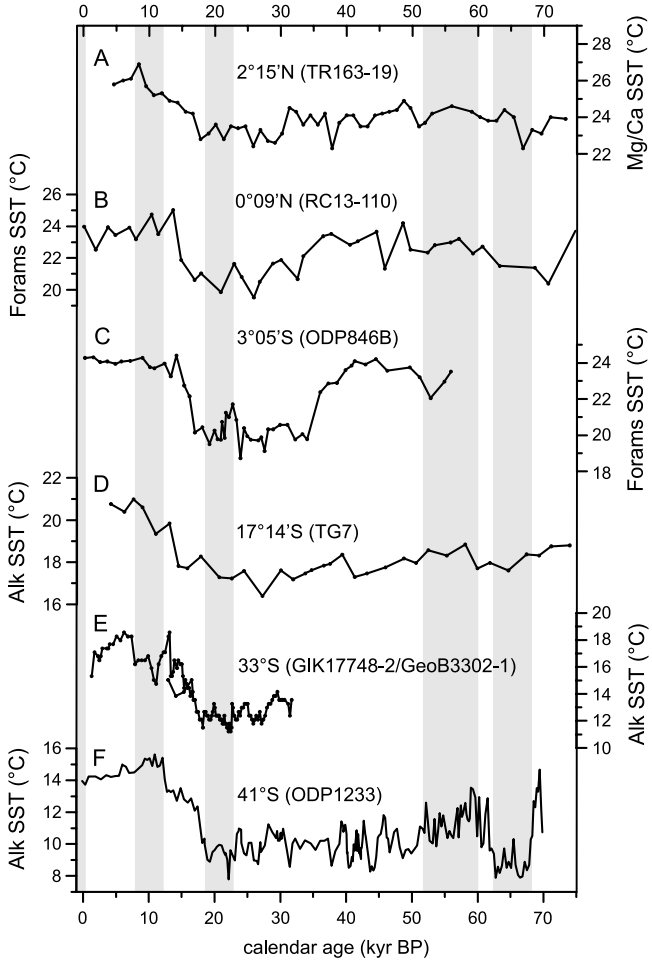

Figure 6. Latitudinal distribution of SST within the Pacific Eastern Boundary Current between 2°N and 41°S. (a) Mg/Ca SST (core TR163-19) [*Lea et al.*, 2000]. (b) SST reconstruction based on planktonic foraminifera fauna distribution (core RC13-110) [*Feldberg and Mix*, 2003]. (c) SST estimation from the planktonic foraminifera assemblage data using the modern analog technique MAT (core ODP846B) [*Martinez et al.*, 2003]. (d) Alkenone-based SST reconstruction (core TG7) [*Calvo et al.*, 2001]. (e) Alkenone-based SST (cores GIK17748-2 and GeoB3302-1) [*Kim et al.*, 2002]. (f) Alkenone-based SST (core ODP1233, this study). The gray bars mark the time intervals as defined for Figure 7 and Table 3: the modern (SST values from *Levitus and Boyer* [1994]), 8–12 kyr (Holocene Climatic Optimum), 19–23 kyr (Last Glacial Maximum), 51–60 kyr (early MIS 3), and 63–68 kyr (MIS 4).

For this purpose, we used our alkenone record at 41°S, two alkenone-based SST reconstructions at 33°S [*Kim et al.*, 2002] and 17°14′S [*Calvo et al.*, 2001], two SST reconstructions based on foraminiferal fauna assemblages at 3°05′S [*Martinez et al.*, 2003] and 0°09′N [*Feldberg and Mix*, 2003], and a Mg/Ca SST reconstruction at 2°15′N [*Lea et al.*, 2000] (see Figure 1 for the location of the cores).

[30] As the records have very different time resolutions, age models (the original age models were used here) and SST proxies, we have focused on the meridional SST gradients in five time intervals defined as follows (Figure 6): the present day [from *Levitus and Boyer*, 1994], the Holocene Climatic Optimum (HCO) (8–12 kyr), the Last Glacial Maximum (LGM) (19–23 kyr), early MIS 3 (51–60 kyr) and MIS 4 (63–68 kyr). In Table 3, we report the values of the present and reconstructed SST gradients, calculated from the mean SSTs for each record and each time interval, and Figure 7 shows the reconstructed SST gradients in the PEBCS for the different time intervals. As the records used here have different SST proxies (alkenone, Mg/Ca and foraminiferal fauna assemblages) with various analytical errors (±0.3 to ±0.5°C, ±0.6°C and ±1 to ±1.8°C respectively; details in publications aforementioned), small SST gradient changes should be considered with caution.

[31] During the coldest intervals, the overall midlatitude-to-equator gradient (2°N–41°S) was around 2.8°C (MIS 2) and 3.7°C (MIS 4) higher than today. Conversely, we observe similar to slightly reduced gradients during the HCO and slightly increased gradients during early MIS 3. The increase in meridional SST gradients during the LGM and MIS 4 is mainly derived from a relatively strong cooling in the southern and central part of the PEBCS (41°–17°S), with particularly enhanced gradients in the southernmost part between ~33°S and 41°S. This is in agreement with modeling results suggesting stronger SST gradients in the midlatitudes at the LGM [*Shin et al.*, 2003a]. In terms of oceanic surface circulation (and linked atmospheric circulation) during the last glacial cold periods (MIS 4 and 2), our SST gradient reconstruction suggests a northward shift of the strong SST gradient area (linked to the ACC) of which the northern limit is nowadays located around 40°S. On the basis of Figure 7, this limit could have been situated around or south of 33°S at the LGM. This would be in the same order of magnitude as the aforementioned ACC northward shift of ~5° in latitude at the LGM in comparison to the present day (see section 5.2). An enhanced northward influence of the ACC up to ~33°S during MIS 2 has also been suggested in paleoproductivity reconstructions along the Chilean coast [*Hebbeln et al.*, 2002; *Mohtadi and Hebbeln*, 2004]. In terms of atmospheric

Table 3. Latitudinal SST Gradients Reconstruction in the Pacific Eastern Boundary Current System for the Five Time Intervals as Defined in Figure 6[a]

Latitudes	Modern	HCO	LGM	Early MIS 3	MIS 4
2°N–41°S	11.2	10.7	14.0	12.6	14.9
0–17°S	3.3	4.1	3.5	4.3	3.4
17°S–41°S	7.2	4.9	8.0	6.9	9.3
0–41°S	10.5	9.0	11.5	11.2	12.7
2°N–0	1.7	1.7	2.5	1.3	2.1
0–3°S	1	0.2	0.3	−0.2	no data
3°S–17°S	2.3	3.9	3.2	4.6	no data
17°S–33°S	4.7	no data	4.9	no data	no data
33°S–41°S	1.5	no data	3.1	no data	no data

[a]Latitudinal SST gradients reconstruction in the Pacific Eastern Boundary Current system for the five time intervals as defined in Figure 6. The values represent the SST differences (in °C) between the different latitudes (left column). Abbreviations are HCO, Holocene Climatic Optimum; LGM, Last Glacial Maximum; and MIS, marine isotope stage.

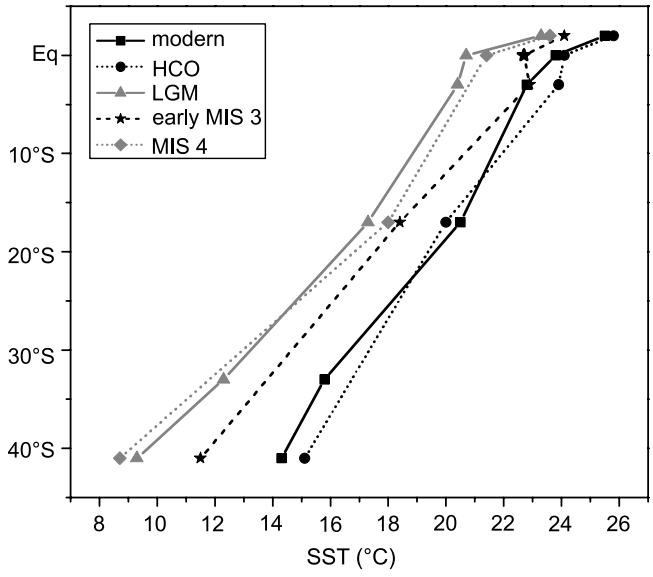

Figure 7. Latitudinal reconstruction of the SST gradients in the Pacific Eastern Boundary Current System during the five time intervals as defined in Figure 6. Figure 7 is based on the mean SSTs for each record and for each period. See Table 3 for the SST gradient values and text for details.

circulation, reconstructions of glaciers movements [*Ammann et al.*, 2001] and humidity changes [*Stuut and Lamy*, 2004] have shown that ~27°S should have been the northernmost limit of the westerlies influence during winter at the LGM. Ultimately, a northward displacement of the westerlies (or their northern boundary), as implied by our results, would be in agreement with the proposed northward shift of the STH at the LGM [e.g., *Andreasen and Ravelo*, 1997; *Mohtadi and Hebbeln*, 2004].

[32] In the low latitudes, previous studies have mentioned an influence of the PCC in the EEP during MIS 2 as MIS 4 [e.g., *Mix et al.*, 1999; *Feldberg and Mix*, 2003; *Martinez et al.*, 2003]. Furthermore, following *Hostetler and Mix* [1999], who have modeled the LGM tropical climate based on a SST field in which lower tropical SSTs than those of CLIMAP are prescribed in the eastern tropical Pacific and equatorial Atlantic Oceans [see *Mix et al.*, 1999], the westward wind flow over northern South America into the Pacific and the tropical Walker circulation were enhanced at the LGM. During cold intervals, we observe similar-than-today SST gradients between 17°S and the equator as well as around the equator (2°N–3°S), within the Equatorial Front, (Figure 7 and Table 3). With this kind of SST gradient configuration, it is not possible to conclude on a stronger (or weaker) circulation in the PEBCS. In comparison to the present day, however, the whole SST distribution was similar to the modern winter pattern (a northward shift of the strong SST gradient area in the south and the presence of the Equatorial Front near the Equator), while the PCC flow is enhanced [*Strub et al.*, 1998]. Therefore our reconstruction would be consistent with a stronger Peru-Chile Current and a cold water tongue extended westward in the low latitudes during MIS 4 and 2, typically a "La Niña-like" pattern as proposed by *Martinez et al.* [2003].

[33] Our SST gradients reconstruction suggests also some interesting pattern for the relatively warm periods (HCO and early MIS 3). During a warmer-than-today climate as the HCO the SST gradients along the whole coast of South America were slightly weaker, especially in the midlatitudes. Consequently the ACC influence through the PCC was weaker, and the associated westerly winds probably situated more poleward. A stronger gradient between 17°S and 3°S could eventually reflect a more southward influence of the equatorial warm waters. Nevertheless, a weaker SST gradient in the south agrees with the previous suggestion of a southward shift of the ACC and the westerlies during the early Holocene (see section 5.2). Finally the SST gradient distribution during early MIS 3 shows an intermediate pattern. Whereas the whole gradient was stronger than present, the latitudinal distribution was different than during MIS 4 and 2, and closer to the HCO distribution.

6. Summary and Conclusions

[34] 1. At a regional scale, the general trends of our SST record are in agreement with paleoenvironmental records from the adjacent continent and previous SST reconstructions that cover the last ~30 kyr, in particular the SST increase of ~6°C over termination I. Other features like a cooling that matches the ACR as defined in Antarctic ice cores are partly inconsistent with land records. Some of these latter results provided evidences for a cooling synchronous with the NH YD cold event whereas our new SST record suggests a pronounced warming of ~2°C during this time interval similar to the Antarctic ice core records.

[35] 2. Our SST record reveals a clear "Antarctic timing" of millennial-scale temperature changes during the last 70 kyr. A comparison to other paleoceanographic records from the SH midlatitudes suggests that these changes occurred quasi hemisphere wide. In addition, coeval changes can be observed in Antarctic dust and sea ice extent records that would be consistent with the following scenario. For SH cold periods, the westerly wind circulation around Antarctica was enhanced and the northern boundary of the westerlies moved equatorward resulting in sea ice export away from Antarctica through an enhanced Ekman drift. Linked to a northward widening of the westerlies, the ACC was displaced northward and advected cold, subantarctic water into the SH midlatitudes. Conversely, during SH warm phases wind intensities decreased, the westerlies and the ACC were more poleward confined and eventually decreased the advection of cold water masses into the midlatitudes. Our scenario for SH millennial-scale changes resembles the observed pattern related to interannual to decadal-scale SH climate modes such as the SAM, suggesting that long-term changes in these modes may ultimately be involved as well. Finally, the clear "Antarctic timing" pattern is consistent with the seesaw mechanism often discussed in relation to NH versus SH millennial-scale climate pattern. However, the consistent temperature pattern around Antarctica in different ocean basins could

also imply a larger involvement or even a source of millennial-scale climate variability in the Southern Hemisphere.

[36] 3. A paleo-SST gradient reconstruction covering the complete latitudinal range of the PEBCS suggests an equatorward displaced subtropical gyre circulation during MIS 2 and 4, similar to the modern winter pattern. This configuration would be mainly linked to an equatorward shift of the northernmost boundary of the ACC resulting in enhanced SST gradients in the southern part of the PEBCS, and to the presence of the Equatorial Front near the equator. Therefore we might suggest that the PCC flow was stronger, that more cold waters of a southern high-latitude origin entered the southeast equatorial Pacific and that the cold tongue was extended westward. Conversely, the oceanic circulation in the PEBCS was probably weakened and the ACC, and associated westerly wind belt, moved southward during relatively warm periods (early MIS 3 and HCO).

[37] **Acknowledgments.** We would like to thank Peter Müller and Ralph Kreutz for help in the laboratory and Marcus Elvert and Enno Schefuss for helpful suggestions on the alkenone preparation and analysis. We further acknowledge Helge Arz and Emmanuel Chapron for helpful discussions and Eva Calvo as well as Xavier Crosta for contributing data. Marco Mohtadi is thanked for suggestions on an earlier version of the manuscript. Two anonymous reviewers provided helpful comments that improved the manuscript. The study was funded by the German Science Foundation through the grant DFG-He-3412-1-3 and was technically supported by the Research Center Ocean Margins (RCOM) in Bremen. This research used samples provided by the Ocean Drilling Program (ODP). The ODP is sponsored by the U.S. National Science Foundation (NSF) and participating countries under management of Joint Oceanographic Institutions (JOI), Inc. This is RCOM publication 0305.

References

Abarzúa, A. M., C. Villagrán, and P. I. Moreno (2004), Deglacial and postglacial climate history in east-central Isla Grande de Chiloe, southern Chile (43°S), *Quat. Res.*, *62*, 49–59.

Ammann, C., B. Jenny, K. Kammer, and B. Messerli (2001), Late Quaternary glacier response to humidity changes in the arid Andes of Chile (18–29°S), *Palaeogeogr. Palaeoclimatol. Palaeoecol.*, *172*, 313–326.

Andreasen, D. J., and A. C. Ravelo (1997), Tropical Pacific Ocean thermocline depth reconstructions for the last glacial maximum, *Paleoceanography*, *12*, 395–413.

Ashworth, A. C., and J. W. Hoganson (1993), The magnitude and rapidity of the climate change marking the end of the Pleistocene in the mid-latitudes of South America, *Palaeogeogr. Palaeoclimatol. Palaeoecol.*, *101*, 263–270.

Basile, I., F. E. Grousset, M. Revel, J. R. Petit, P. E. Biscaye, and N. I. Barkov (1997), Patagonian origin of glacial dust deposited in East Antarctica (Vostok and Dome C) during glacial stages 2, 4 and 6, *Earth Planet. Sci. Lett.*, *146*, 573–589.

Benn, D. I., and C. M. Clapperton (2000), Glacial sediment-landform associations and paleoclimate during the last glaciation, Strait of Magellan, Chile, *Quat. Res.*, *54*, 13–23.

Bennett, K. D., S. G. Haberle, and S. H. Lumley (2000), The Last Glacial-Holocene transition in southern Chile, *Science*, *290*, 325–328.

Berger, W., K. Fischer, C. Lai, and G. Wu (1987), Ocean productivity and organic carbon flux. part I. Overview and maps of primary production and export production, *SIO Tech. Rep. Ref. Ser. 87-30*, Scripps Inst. of Oceanogr., Univ. of Calif., La Jolla.

Blunier, T., and E. J. Brook (2001), Timing of millennial-scale climate change in Antarctica and Greenland during the last glacial period, *Science*, *291*, 109–112.

Brathauer, U., and A. Abelmann (1999), Late Quaternary variations in sea surface temperatures and their relationship to orbital forcing recorded in the Southern Ocean (Atlantic sector), *Paleoceanography*, *14*, 135–148.

Broecker, W. S. (1998), Paleocean circulation during the last deglaciation: A bipolar seesaw?, *Paleoceanography*, *13*, 119–121.

Calvo, E., C. Pelejero, J. C. Herguera, A. Palanques, and J. O. Grimalt (2001), Insolation dependence of the southeastern subtropical Pacific Sea surface temperature over the last 400 kyrs, *Geophys. Res. Lett.*, *28*, 2481–2484.

Cerveny, R. (1998), Present climates of South America, in *Climates of the Southern Continents: Present, Past and Future*, edited by J. E. Hobbs et al., pp. 107–135, John Wiley, Hoboken, N. J.

Charles, C. D., J. Lynch-Stieglitz, U. S. Ninnemann, and R. G. Fairbanks (1996), Climate connections between the hemisphere revealed by deep sea sediment core/ice core correlations, *Earth Planet. Sci. Lett.*, *142*, 19–27.

COHMAP Members, M. (1988), Climatic changes of the last 18,000 years: Observations and model simulations, *Science*, *241*, 1043–1052.

Comiso, J. C. (2003), Large-scale characteristics and variability of the global sea-ice cover, in *Sea Ice: An Introduction to its Physics, Chemistry, Biology, and Geology*, edited by D. N. Thomas and G. S. Diekmann, pp. 112–142, Blackwell, Malden, Mass.

Delmonte, B., J. Petit, and V. Maggi (2002), Glacial to Holocene implications of the new 27000-year dust record from the EPICA Dome C (East Antarctica) ice core, *Clim. Dyn.*, *18*(8), 647–660, doi:10.1007/s00382-001-0193-9.

Denton, G. H., C. J. Heusser, T. V. Lowell, P. I. Moreno, B. G. Andersen, L. E. Heusser, C. Schluchter, and D. R. Marchant (1999a), Interhemispheric linkage of paleoclimate during the last glaciation, *Geogr. Ann., Ser. A*, *81*, 107–153.

Denton, G. H., T. V. Lowell, C. J. Heusser, C. Schluchter, B. G. Andersen, L. E. Heusser, P. I. Moreno, and D. R. Marchant (1999b), Geomorphology, stratigraphy, and radiocarbon chronology of Llanquihue drift in the area of the southern Lake District, Seno Reloncavi, and Isla Grande de Chiloe, Chile, *Geogr. Ann., Ser. A*, *81*, 167–229.

EPICA Community Members (2004), Eight glacial cycles from an Antarctic ice core, *Nature*, *429*, 623–628.

Feldberg, M. J., and A. C. Mix (2003), Planktonic foraminifera, sea surface temperatures, and mechanisms of oceanic change in the Peru and south equatorial currents, 0–150 ka BP, *Paleoceanography*, *18*(1), 1016, doi:10.1029/2001PA000740.

Fonseca, T. (1989), An overview of the Poleward Undercurrent and upwelling along the Chilean coast, in *Poleward Flows Along Eastern Ocean Boundaries*, S. J. Neshyba et al., pp. 203–228, Springer, New York.

Ganopolski, A., and S. Rahmstorf (2001), Rapid changes of glacial climate simulated in coupled climate model, *Nature*, *409*, 153–158.

Ganopolski, A., S. Rahmstorf, V. Petoukhov, and M. Claussen (1998), Simulation of modern and glacial climates with a coupled global model of intermediate complexity, *Nature*, *391*, 351–356.

Gersonde, R., X. Crosta, A. Abelmann, and L. Armand (2005), Sea-surface temperature and sea ice distribution of the Southern Ocean at the EPILOG Last Glacial Maximum—A circum-Antarctic view based on siliceous microfossil records, *Quat. Sci. Rev.*, *24*(7–9), 869–896, doi:10.1016/j.quascirev.2004.07.015.

Glasser, N. F., S. Harrison, V. Winchester, and M. Aniya (2004), Late Pleistocene and Holocene palaeoclimate and glacier fluctuations in Patagonia, *Global Planet. Change*, *43*, 79–101.

Grousset, F. E., P. E. Biscaye, M. Revel, J.-R. Petit, K. Pye, S. Joussaume, and J. Jouzel (1992), Antarctic (Dome C) ice-core dust at 18 ky BP: Isotopic constraints on origins, *Earth Planet. Sci. Lett.*, *111*, 175–182.

Haberle, S. G., and K. D. Bennett (2004), Postglacial formation and dynamics of north Patagonian rainforest in the Chonos Archipelago, southern Chile, *Quat. Sci. Rev.*, *23*(23–24), 2433–2452, doi:10.1016/j.quascirev.2004.03.001.

Hajdas, I., G. Bonani, P. I. Moreno, and D. Ariztegui (2003), Precise radiocarbon dating of Late-Glacial cooling in mid-latitude South America, *Quat. Res.*, *59*(1), 70–78, doi:10.1016/S0033-5894(02)00017-0.

Hall, A., and M. Visbeck (2002), Synchronous variability in the Southern Hemisphere atmosphere, sea ice, and ocean resulting from the annular mode, *J. Clim.*, *15*(21), 3043–3057, doi:10.1175/1520-0442(2002)015<3043:SVITSH>2.0.CO;2.

Hebbeln, D., M. Marchant, and G. Wefer (2002), Paleoproductivity in the southern Peru-Chile Current through the last 33,000 years, *Mar. Geol.*, *186*(3–4), 487–504, doi:10.1016/S0025-3227(02)00331-6.

Heusser, C. J. (1989), Southern westerlies during the Last Glacial Maximum, *Quat. Res.*, *31*, 423–425.

Heusser, C. J., L. E. Heusser, T. V. Lowell, A. Moreira, and S. Moreira (2000), Deglacial palaeoclimate at Puerto del Hambre, subantarctic Patagonia, Chile, *J. Quat. Sci.*, *15*(1), 101–114.

Hostetler, S. W., and A. C. Mix (1999), Reassessment of ice-age cooling of the tropical ocean and atmosphere, *Nature*, *399*, 673–676.

Hulton, N. R. J., R. S. Purves, R. D. McCulloch, D. E. Sugden, and M. J. Bentley (2002), The Last Glacial Maximum and deglaciation in southern South America, *Quat. Sci. Rev.*, *21*, 233–241.

Jouzel, J., et al. (1995), The 2-step shape and timing of the last deglaciation in Antarctica, *Clim. Dyn.*, *11*, 151–161.

Kanfoush, S. L., D. A. Hodell, C. D. Charles, T. P. Guilderson, P. G. Mortyn, and U. S. Ninnemann (2000), Millennial-scale instability of the Antarctic ice sheet during the last glaciation, *Science*, *288*, 1815–1818.

Kanfoush, S., D. Hodell, C. Charles, J. Stoner, J. Channell, and P. G. Morthyn (2003), Correlation of ice-rafted detritus in South Atlantic sediments with polar-ice: Implications for interhemispheric millennial climate changes during the Last Glacial Period, paper presented at Annual Meeting, Geol. Soc. of Am., Seattle, Wash.

Kim, J. H., R. R. Schneider, D. Hebbeln, P. J. Müller, and G. Wefer (2002), Last deglacial sea-surface temperature evolution in the southeast Pacific compared to climate changes on the South American continent, *Quat. Sci. Rev.*, *21*, 2085–2097.

Knorr, G., and G. Lohmann (2003), Southern Ocean origin for the resumption of Atlantic thermohaline circulation during deglaciation, *Nature*, *424*, 532–536.

Koutavas, A., J. Lynch-Stieglitz, T. M. Marchitto Jr., and J. P. Sachs (2002), El Niño-like pattern in ice age tropical Pacific sea surface temperature, *Science*, *297*, 226–230.

Krinner, G., and C. Genthon (2003), Tropospheric transport of continental tracers towards Antarctica under varying climatic conditions, *Tellus, Ser. B*, *55*, 54–70.

Lamy, F., D. Hebbeln, and G. Wefer (1998), Late Quaternary precessional cycles of terrigenous sediment input off the Norte Chico, Chile (27.5 degrees S) and palaeoclimatic implications, *Palaeogeogr. Palaeoclimatol. Palaeoecol.*, *141*, 233–251.

Lamy, F., D. Hebbeln, U. Rohl, and G. Wefer (2001), Holocene rainfall variability in southern Chile: A marine record of latitudinal shifts of the southern westerlies, *Earth Planet. Sci. Lett.*, *185*, 369–382.

Lamy, F., C. Rühlemann, D. Hebbeln, and G. Wefer (2002), High- and low-latitude climate control on the position of the southern Peru-Chile Current during the Holocene, *Paleoceanography*, *17*(2), 1028, doi:10.1029/2001PA000727.

Lamy, F., J. Kaiser, U. Ninnemann, D. Hebbeln, H. Arz, and J. Stoner (2004), Antarctic timing of surface water changes off Chile and Patagonian ice sheet response, *Science*, *304*, 1959–1962.

Lea, D. W., D. K. Pak, and H. J. Spero (2000), Climate impact of late Quaternary equatorial Pacific sea surface temperature variations, *Science*, *289*, 1719–1724.

Levitus, S., and T. Boyer (1994), *World Ocean Atlas 1994*, vol. 4, *Temperature*, *NOAA Atlas NESDIS 4*, 129 pp., Natl. Oceanic and Atmos. Admin., Silver Spring, Md.

Liu, Z. Y., S. I. Shin, B. Otto-Bliesner, J. E. Kutzbach, E. C. Brady, and D. E. Lee (2002), Tropical cooling at the Last Glacial Maximum and extratropical ocean ventilation, *Geophys. Res. Lett.*, *29*(10), 1409, doi:10.1029/2001GL013938.

Lowell, T. V., C. J. Heusser, B. G. Andersen, P. I. Moreno, A. Hauser, L. E. Heusser, C. Schlüchter, D. R. Marchant, and G. H. Denton (1995), Interhemispheric correlation of late Pleistocene glacial events, *Science*, *269*, 1541–1549.

Lund, S. P., J. Stoner, and F. Lamy (2005), Late Quaternary paleomagnetic secular variation records and chronostratigraphy from ODP Sites 1233 and 1234, *Proc. Ocean Drill. Program Sci. Results*, in press.

Markgraf, V., J. R. Dodson, P. A. Kershaw, M. S. McGlone, and N. Nicholls (1992), Evolution of late Pleistocene and Holocene climates in the circum-South Pacific land areas, *Clim. Dyn.*, *6*, 193–211.

Martinez, I., L. Keigwin, T. T. Barrows, Y. Yokoyama, and J. Southon (2003), La Niña-like conditions in the eastern equatorial Pacific and a stronger Choco jet in the northern Andes during the last glaciation, *Paleoceanography*, *18*(2), 1033, doi:10.1029/2002PA000877.

Mashiotta, T. A., D. W. Lea, and H. J. Spero (1999), Glacial-interglacial changes in Subantarctic sea surface temperature and δO^{18}-water using foraminiferal Mg, *Earth Planet. Sci. Lett.*, *170*, 417–432.

Massaferro, J., and S. J. Brooks (2002), Response of chironomids to late Quaternary environmental change in the Taitao Peninsula, southern Chile, *J. Quat. Sci.*, *17*, 101–111.

Masson, V., et al. (2000), Holocene climate variability in Antarctica based on 11 ice-core isotopic records, *Quat. Res.*, *54*, 348–358.

Mix, A. C., A. E. Morey, N. G. Pisias, and S. W. Hostetler (1999), Foraminiferal faunal estimates of paleotemperature: Circumventing the no-analog problem yields cool ice age tropics, *Paleoceanography*, *14*, 350–359.

Mix, A. C., R. Tiedemann, P. Blum, and Shipboard Scientists (2003), *Leg 202 Summary*, 145 pp., Ocean Drill. Program, College Station, Tex.

Mohtadi, M., and D. Hebbeln (2004), Mechanisms and variations of the paleoproductivity off northern Chile (24°S–33°S) during the last 40,000 years, *Paleoceanography*, *19*, PA2023, doi:10.1029/2004PA001003.

Mollenhauer, G., M. Kienast, F. Lamy, H. Meggers, R. R. Schneider, J. M. Hayes, and T. I. Eglinton (2005), An evaluation of ^{14}C age relationships between co-occurring foraminifera, alkenones, and total organic carbon in continental margin sediments, *Paleoceanography*, *20*, PA1016, doi:10.1029/2004PA001103.

Moreno, P. I. (2004), The last transition from extreme glacial to extreme interglacial climate in NW Patagonia: Regional and global implications, *Eos Trans. AGU*, *85*(47), Fall Meet. Suppl., Abstract GC53A-02.

Moreno, P. I., and A. L. León (2003), Abrupt vegetation changes during the Last Glacial to Holocene transition in mid-latitude South America, *J. Quat. Sci.*, *18*, 787–800.

Moreno, P. I., G. L. Jacobson, T. V. Lowell, and G. H. Denton (2001), Interhemispheric climate links revealed by a late-glacial cooling episode in southern Chile, *Nature*, *409*, 804–808.

Müller, P. J., G. Kirst, G. Ruhland, I. von Storch, and A. Rosell-Mele (1998), Calibration of the alkenone paleotemperature index $UK'37$ based on core-tops from the eastern South Atlantic and the global ocean (60°N–60°S), *Geochim. Cosmochim. Acta*, *62*, 1757–1772.

Ninnemann, U. S., and C. D. Charles (1997), Regional differences in Quaternary Subantarctic nutrient cycling: Link to intermediate and deep water ventilation, *Paleoceanography*, *12*, 560–567.

Ninnemann, U. S., C. Charles, and D. Hodell (1999), Origin of global millennial scale climate events: Constraints from the Southern Ocean deep sea sedimentary record, in *Mechanisms of Global Climate Change at Millennial Time Scales*, *Geophys. Monogr. Ser.*, vol. 112, edited by P. U. Clark et al., pp. 94–112, AGU, Washington, D. C.

Pahnke, K., R. Zahn, H. Elderfield, and M. Schulz (2003), 340,000-year centennial-scale marine record of Southern Hemisphere climatic oscillation, *Science*, *301*, 948–952.

Petit, J. R., M. Briat, and A. Royer (1981), Ice Age aerosol content from East Antarctic ice core samples and past wind strength, *Nature*, *343*, 391–394.

Prahl, F. G., and S. G. Wakeham (1987), Calibration of unsaturation patterns in long-chain ketone compositions for paleotemperature assessment, *Nature*, *330*, 367–369.

Prahl, F. G., L. A. Muehhausen, and D. L. Zahnle (1988), Further evaluation of long-chain alkenones as indicators of paleoceanographic conditions, *Geochim. Cosmochim. Acta*, *52*, 2303–2310.

Rahmstorf, S. (2002), Ocean circulation and climate during the past 120,000 years, *Nature*, *419*, 207–214.

Rothlisberger, R., R. Mulvaney, E. W. Wolff, M. A. Hutterli, M. Bigler, S. Sommer, and J. Jouzel (2002), Dust and sea salt variability in central East Antarctica (Dome C) over the last 45 kyrs and its implications for southern high-latitude climate, *Geophys. Res. Lett.*, *29*(20), 1963, doi:10.1029/2002GL015186.

Rutter, N. W., A. J. Weaver, D. Rokosh, A. F. Fanning, and D. G. Wright (2000), Data-model comparison of the Younger Dryas event, *Can. J. Earth Sci.*, *37*, 811–830.

Schmittner, A., O. A. Saenko, and A. J. Weaver (2003), Coupling of the hemispheres in observations and simulations of glacial climate change, *Quat. Sci. Rev.*, *22*, 659–671.

Shaffer, G., S. Hormazabal, O. Pizarro, and M. Ramos (2004), Circulation and variability in the Chile Basin, *Deep Sea Res., Part I*, *51*(10), 1367–1386, doi:10.1016/j.dsr.2004.05.006.

Shemesh, A., D. Hodell, X. Crosta, S. Kanfoush, C. Charles, and T. Guilderson (2002), Sequence of events during the last deglaciation in Southern Ocean sediments and Antarctic ice cores, *Paleoceanography*, *17*(4), 1056, doi:10.1029/2000PA000599.

Shin, S. I., Z. Liu, B. Otto-Bliesner, E. C. Brady, J. E. Kutzbach, and S. P. Harrison (2003a), A simulation of the Last Glacial Maximum climate using the NCAR-CCSM, *Clim. Dyn.*, *20*, 127–151.

Shin, S.-I., Z. Liu, B. L. Otto-Bliesner, J. E. Kutzbach, and S. J. Vavrus (2003b), Southern Ocean sea-ice control of the glacial North Atlantic thermohaline circulation, *Geophys. Res. Lett.*, *30*(2), 1096, doi:10.1029/2002GL015513.

Shulmeister, J., et al. (2004), The Southern Hemisphere westerlies in the Australasian sec-

tor over the last glacial cycle: A synthesis, *Quat. Int.*, *118–119*, 23–53.

Stocker, T. F. (1998), Climate change—The seesaw effect, *Science*, *282*, 61–62.

Streten, N. A., and J. W. Zillman (1984), Climate of the South Pacific, in *Climates of the Oceans*, edited by H. van Loon, pp. 26–429, Elsevier, New York.

Strub, P. T., J. M. Mesias, V. Montecino, J. Ruttlant, and S. Salinas (1998), Coastal ocean circulation off western South America, in *The Global Coastal Ocean: Regional Studies and Syntheses*, edited by A. R. Robinson and K. H. Brink, pp. 273–315, John Wiley, New York.

Stuut, J.-B. W., and F. Lamy (2004), Climate variability at the southern boundaries of the Namib (southwestern Africa) and Atacama (northern Chile) coastal deserts during the last 120,000 yr, *Quat. Res.*, *62*, 301–309.

Thompson, D. W. J., and J. M. Wallace (2000), Annular modes in the extratropical circulation. part I: Month-to-month variability, *J. Clim.*, *13*, 1000–1016.

Thompson, D. W. J., J. M. Wallace, and G. C. Hegerl (2000), Annular modes in the extratropical circulation. part II: Trends, *J. Clim.*, *13*, 1018–1036.

Thompson, L. G., E. Mosley-Thompson, M. E. Davis, P.-N. Lin, K. A. Hendersen, J. Cole-Dai, J. F. Bolzan, and K.-B. Liu (1995), Late glacial stage and Holocene tropical ice core records from Huascaran, Peru, *Science*, *269*, 46–50.

Trenberth, K. E. (1991), Storm tracks in the Southern Hemisphere, *J. Atmos. Sci.*, *48*, 2159–2178.

Voelker, A. H. L. (2002), Global distribution of centennial-scale records for Marine Isotope Stage (MIS) 3: A database, *Quat. Sci. Rev.*, *21*, 1185–1212.

Wardle, R. (2003), Using anticyclonicity to determine the position of the Southern Hemisphere westerlies: Implications for the LGM, *Geophys. Res. Lett.*, *30*(23), 2200, doi:10.1029/2003GL018792.

Weaver, A. J., O. A. Saenko, P. U. Clark, and J. X. Mitrovica (2003), Meltwater pulse 1A from Antarctica as a trigger of the Bølling-Allerød warm interval, *Science*, *299*, 1709–1713.

Wyrtki, K. (1965), Oceanography of the eastern equatorial Pacific Ocean, *Oceanogr. Mar. Biol.*, *4*, 33–68.

Wyrwoll, K.-H., B. Dong, and P. Valdes (2000), On the position of Southern Hemisphere westerlies at the Last Glacial Maximum: An outline of AGCM simulation results and evaluation of their implications, *Quat. Sci. Rev.*, *19*, 881–898.

D. Hebbeln and J. Kaiser, Deutsche Forschung Gemeinschaft Research Center Ocean Margins, University of Bremen, Leobener Strasse, 28359 Bremen, Germany. (kaiserj@uni-bremen.de)

F. Lamy, GeoForschungsZentrum-Potsdam, Telegrafenberg, 14473 Potsdam, Germany.